JOURNAL OF CATALYSIS 123, 319–332 (1990)

Preparation and Characterization of $Pt(RuO_2)/TiO_2$ Catalysts: Test in a Continuous Water Photolysis System

J. C. ESCUDERO, S. CERVERA-MARCH, J. GIMÉNEZ, AND R. SIMARRO

Department of Chemical Engineering, University of Barcelona, Martí i Franqués, 1, 6, Barcelona 08028, Spain

Received July 13, 1988; revised June 7, 1989

Aqueous suspensions of $Pt(RuO_2)/TiO_2$ photocatalysts, where Pt has been reduced by different techniques, have been irradiated with UV light in a photoreactor with a continuous gas phase composed of Ar and photoproducts. The performance of the catalysts in the water-splitting process has been related to these different Pt reduction methods by consideration of the physical characteristics of the powders (deposits and support), such as crystal structure, specific surface area, particle size, quality of the metal dispersion, as well as the oxidation state and doping changes brought about by these techniques. Long-term activity could be studied given the nature of the photoreactor system used, where photoproducts do not build up and steady conditions can be reached. The catalytic role of RuO_2 has been specifically studied in connection with the preparative treatments followed. © 1990 Academic Press, Inc.

INTRODUCTION

A large number of methods have been presented in recent years with a view to carrying out the water photolysis process (*1–4*). Using different radiation sources, several types of photocatalyst have been tested. The most frequently used catalysts have been semiconductors loaded (or not) with metals or metallic oxides. When the photolysis process was carried out without sacrificial agents, one of the most used semiconductors was TiO_2.

These catalysts have been prepared and characterized by various techniques (*5, 6*), which permit one to relate the preparative method used with the results obtained in the catalytic testing. However, the characterization of a photocatalyst is somewhat different from the characterization of a conventional one. In general catalysis, activity is ascribed mainly to the surface (internal and external) of the catalyst, while in photocatalysis, the fact of shadowing and backscattering might be crucial, for the light intensity profiles generated by suspensions of solid particles can attenuate differences in productivity corresponding to catalysts with different activity.

Characterization alone does not give all the information about the catalyst behavior in the water photolysis process. The experimental device used in the catalyst testing and the operating conditions are also very important. Several characteristics of the system used in the water cleavage must be considered, such as photoreactor type, radiation source, and the fluid dynamics of the system.

Most water photolysis experiments involving aqueous suspensions of photocatalysts described in the literature have been carried out in small batch reactors. These devices only allow the study of the system in nonsteady state. The character of this nonsteady state in photocatalysis is very complex, because there are many factors affecting the dynamic response of the catalyst–reactor system which are very different in nature. In addition, not enough attention is paid to radiation parameters, such as lamp position, radiation model, and geometry of the system. Other variables, such as temperature, partial pressure of photoprod-

0021-9517/90 $3.00

ucts, and outer atmosphere composition, play a role in the evolution of the process and thus should be carefully controlled.

A slurry batch reactor with a continuous gas phase was used in this work to carry out the water photolysis experiments. This experimental device allows one to study the change in hydrogen production rate with time and to control the most important variables playing a role in the water cleavage process. Also, in such a system it is possible to study the activity changes of the catalyst during the test period.

TiO_2 will be referred to as "the support," although from the photocatalysis point of view it behaves as an active material, pumping electrons and holes to the solid surface under the effect of light. The catalytic material used in this study was TiO_2 loaded with RuO_2 and/or Pt. The metal loading was made by three different methods. The catalysts prepared were characterized by several techniques in order to obtain different data which permit us to explain their catalytic behavior. The catalysts were tested in the water photolysis process using a continuous flow device.

METHODS

(*i*) *Catalyst Preparation*

The semiconductor used as catalytic support was TiO_2 (Aldrich, anatase powder). Two different types of catalyst were prepared: monofunctional catalysts, where TiO_2 was loaded with Pt, and bifunctional catalysts, where TiO_2 was loaded with Pt and RuO_2.

The RuO_2/TiO_2 powder was prepared by impregnation of TiO_2 with a solution of $RuCl_3 \cdot 3H_2O$ (Aldrich). A solution obtained by dissolving 200 mg of $RuCl_3 \cdot 3H_2O$ in 7 ml of water was added, dropwise, to 8 g of powdered titania to form a slurry. This slurry was introduced in an oven with programmed temperature. The initial temperature was 50°C and it reached 350°C at a rate of 5°C/min. The oxidation of Ru(III) was carried out at this temperature (350°C) during 15 h, the final product obtained being RuO_2/TiO_2. The weight percent of Ru in the sample was 1%. This preparation method was analogous to others described in the literature (*7–11*) although different methods are also described (*12–17*).

The Pt loading was carried on the RuO_2/TiO_2 powder in the case of bifunctional catalysts or on titania alone in the case of monofunctional catalysts. Three different methods were used to deposit Pt (from $H_2PtCl_6 \cdot xH_2O$, Aldrich) on the powders:

(1) Reduction of Pt by citrates (*18, 19*). Sodium citrate (215 mg) and H_2PtCl_6 (7.8 ml) standard solution, containing 1.34 mg H_2PtCl_6/ml solution, were dissolved in 100 ml of water. The resulting solution was heated for 4 h at 90°C in a flask with continuous stirring. Then 1 g of support was introduced and the suspension was sonicated. Finally, the addition of HCl produced flocculation of the catalyst, which was separated from the liquid by centrifugation and subsequent washing until no Cl^- could be detected (no precipitate or turbidity was formed when silver nitrate was added to the washing water).

(2) Hydrogenation at 400°C (*20, 21*). The support was impregnated with H_2PtCl_6 and afterward reduced with hydrogen. Thus, 6.4 ml of standard solution of H_2PtCl_6 (1.34 mg/ml) was added, dropwise, to 1 g of support to form a slurry. This slurry was introduced in an oven for 25 h at 110°C. The dried powder obtained was ground and introduced into a hydrogenation reactor, where it was heated from room temperature to 400°C. During the heating process a stream of N_2 gas (1.3 ml/s) was passed continuously through the reactor. When the working temperature (400°C) was reached, the N_2 was substituted by a H_2 stream (1.3 ml/s). This stream was passed through the reactor for 7 h to ensure Pt(IV) reduction. The reactor was then cooled in a nitrogen stream and the preparation of the catalyst finished.

(3) Photoplantinization (*22–25*). The Pt was loaded by photoreduction of Pt(IV)

without any sacrificial agents. Standard solution of H_2PtCl_6 (0.45 ml) was added to 75 mg of support suspended in 150 ml of water. This suspension was placed in the experimental device where photolysis experiments were carried out. Then, the suspension was irradiated, forming the final catalyst after a few minutes of irradiation. The catalysts thus prepared were tested *in situ*, that is, without further manipulation of the powders. In the cases where a characterization or storage of these catalysts was required, they were separated from the liquid by filtration.

The different catalysts will be referred to in a condensed notation, giving information about the support type, catalytic formulation, and preparative method used. The catalysts prepared are shown in Table 1.

(*ii*) *Catalyst Characterization*

XRD analysis was made with a Siemens D-500 powder diffractometer to study the crystal structure of the titania support. The catalyst texture was determined by physical adsorption and the specific surface area was calculated by using the BET method. The physical adsorption was measured using a Micromeritics Accusorb 2100E volumetric apparatus with N_2 as adsorbate at 77 K.

Micrographs were made with a Philips EM 301 transmission electron microscope working at 80 or 100 kV. The processing and analysis of the TEM micrographs was carried out in an image analyzer (Kontron Ibas II, Carl Zeiss) to obtain the diameter of the projected area of the particles. This permits the determination of primary-particle size distribution (*26–28*). A sedigraph particle size analyzer (SediGraph from Micromeritics) and SEM image analysis were used to measure agglomerate sizes.

TABLE 1

Catalysts Prepared and Tested

Support	Platinized	Pt reduction	Notation
Titania (T) + RuO_2 (R)[a]	Yes (P)[b]	Citrates (C)	TRP.C
T + R	P	Hydrogenation (H)	TRP.H
T + R	P	Photoplatinization (F)	TRP.F
T	P	C	TP.C
T	P	H	TP.H
T	P	F	TP.F
T + R	No	—	TR
T + R	No	—	TR.H[c]
T	No	—	T.H[c]

[a] 1% Ru.
[b] 0.4% Pt.
[c] Hydrogenation of the support was performed.

The quantity of platinum loaded on the support was determined in the catalysts prepared. When the preparative method used was the impregnation of support with H_2PtCl_6 and reduction with hydrogen (method 2), it was assumed that all the Pt added had been loaded on the support. For the other preparative methods, the determination of Pt percentage was made by photometric measure (*29*). The nonreduced or nonadsorbed H_2PtCl_6 was complexed with $SnCl_2 \cdot 2H_2O$ in acid medium (HCl). The absorbance of the colored complex formed was measured at 403 nm in a Beckman Model 25 spectrophotometer. This permits the calculation of the Pt concentration in the complex solution and, by difference, the Pt loaded on the catalyst. In all the cases presented here, the Pt loading resulted in 0.4% by weight, and RuO_2 was 1%.

The RuO_2 and Pt dispersions on the support surface were observed by TEM. Hydrogen chemisorption permits one to express the metal dispersion on the support surface in terms of the atomic ratio of hydrogen to metal (H/*M*). The equipment used for chemisorption was the same as that used for physical adsorption. To determine the hydrogen-to-metal ratio, all the samples were pretreated by the low-temperature reduction (LTR) method described by Tauster *et al.* (*20*) to avoid the effect of strong metal–support interaction (SMSI). For the catalysts prepared by hydrogen reduction at 400°C (TRP.H and TP.H), the samples were previously oxidized in air at 400°C, to avoid also the SMSI

effects, and then the standard (LTR) pretreatment was applied.

(*iii*) *Experimental Device for Continuous Photolysis*

The photolysis experiments were carried out in a three-phase (S-L-G) photoreactor, with a liquid volume of 300 ml and a gas volume of 300 ml, continuous with respect to the gas phase, already described in detail (*30, 31*). The flow diagram is shown in Fig. 1. An annular photoreactor was placed in an inert (nitrogen) housing, to avoid the negative influence of outer oxygen on process evolution (*32, 33*). An inert gas (Ar) was fed continuously to the reaction chamber, which facilitated the suspension of the catalyst and the variation in the partial pressure of photoproducts, by varying the Ar flow. The effluent gas was partly recycled to the reactor by a membrane pump, and the remainder was allowed to flow out and be continuously analyzed by a gas chromatograph (GC) HP5840A with a gas injection valve.

The experimental conditions used were the same in all the experiments in order to make comparisons meaningful. In all cases the system was purged for 2 h with an Ar stream (2 ml/s) before the experiment. The reactor temperature, catalyst concentration, and recycle gas flow rate were 52 ± 1°C, 0.503 ± 0.003 g/liter, and 22 ± 3 ml/s, respectively. The outgoing gas flow rate was kept constant in the range 0.1–0.5 ml/s.

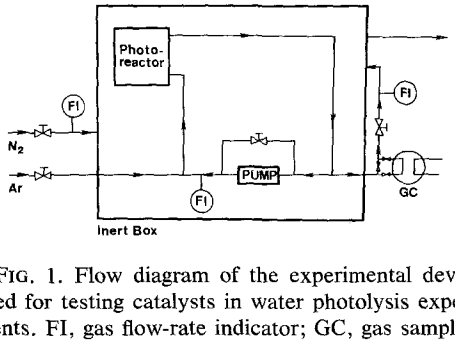

FIG. 1. Flow diagram of the experimental device used for testing catalysts in water photolysis experiments. FI, gas flow-rate indicator; GC, gas sampling valve of gas chromatograph.

Previously, it was proved that the outgoing gas flow rate did not have any influence on the hydrogen production rate in the range employed (*30, 34*). The working pH was neutral.

The energy source was a Hg-vapor UV lamp (Philips HPK 125 W) and the photon flux reaching the reaction chamber with an energy greater than TiO_2 band gap was 1.82×10^{-5} einstein/s (*35*).

RESULTS

(*i*) *Catalyst Characterization*

XRD analysis showed that the titania support used was a mixture of anatase and rutile. The method of Chung (*36*) was used to assess that the anatase content was 99% in weight. The presence of RuO_2 was also observed in the diffractograms when bifunctional catalysts were characterized. The characteristic peaks of Pt were not observed in these diagrams, probably due to the low concentration of Pt and to the reduced dimension of its crystallites.

It was observed that the shape of the characteristic adsorption–desorption isotherm of the titania support corresponds to Type II in the BDDT classification (*26*), which indicates that the support is a nonporous solid. This technique establishes that the various preparative methods were without influence on the specific surface area of the catalysts, which in each case was 10 m^2/g.

The primary particle size distribution obtained by TEM analysis corresponds to the log-normal type (*26–28*) with a geometrical mean of 131 nm and a standard deviation of 0.346 for the logarithm. This implies a mean diameter of 138 nm.

The cumulative mass percent distribution based upon the Stokesian or equivalent spherical diameter of agglomerates was measured by sedigraphy. Figure 2 shows the different distributions obtained for the support agglomerates dispersed in water by mechanical stirring (left line) and by sonication (right line), and for all the catalysis dispersed by sonication (shadowed zone). It

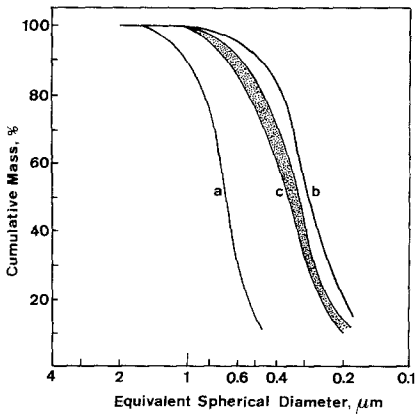

FIG. 2. Agglomerate Stokesian diameter distributions measured by X-ray sedigraphy. (a) TiO_2, after mechanical stirring; (b) TiO_2, after sonication; and (c) all the catalysts prepared (see Table 1), after sonication.

can be observed that the agglomerate distribution is analogous in all the catalysts prepared and, consequently, is independent of the preparative methods. This fact is crucial for this study, since from a fluid dynamic point of view, the behavior of the different catalysts will be the same in all cases, for the relative fluid–solid velocity will remain constant. Hence, the mass transfer phenomena associated with the flow of fluids will have the same extension for all the prepared catalysts. From the radiation point of view, the extent of light scattering originated by the solids in suspension will be the same in every case. It has already been pointed out (*37*) that depending on the nature of the titania used as support, the agglomerate size distribution is affected by the preparative method used, and this can induce considerable variations in hydrogen productivity.

Sedigraphy is only useful for agglomerates with diameters larger than ca. 200 nm. Thus, to obtain a more accurate estimate of the agglomerate size distributions, SEM was applied together with image analysis. For TRP.C catalysts a log-normal distribution was obtained, with a geometrical mean of 323 nm and a standard deviation of 0.453 of the logarithm. This leads to a mean aggregate diameter of 355 nm, in agreement with the sedigraphy results. For the other catalysts prepared, this technique was not used because X-ray sedimentation had shown that all these catalysts presented a similar distribution.

Micrographs of the titania support confirm that it is a nonporous solid, with particles having a rounded shape and uniform surface (see Fig. 3a). When TR particles were analyzed by TEM, it was observed that RuO_2 deposits appeared as agglomerates on the surface of the support (see Fig. 3b), which shows that the dispersion of metallic oxide is not homogeneous. In the case of TRP-type catalyst, the Pt deposits were not observed in addition to the presence of RuO_2 islets (see Fig. 3c).

Figures 3d, 3e, and 3f show, respectively, the TEM images of TP.C, TP.H, and TP.F catalysts. In this case, the interference of RuO_2 does not exist. For the TP.H catalysts, the presence of large Pt aggregates on the support surface was observed, which indicates that this method does not produce a good dispersion of the metal. When TP.C and TP.F catalysts were analyzed, the presence of large metallic aggregates was not observed, which shows that these preparative methods give a better dispersion of the metal.

The results obtained by hydrogen chemisorption are shown in Table 2 and they are consistent with those observed by TEM concerning the quality of metal dispersions.

(*ii*) *Water Photolysis*

The first step was to test the photoactivity of titania itself. It was observed that after 2 h of irradiation there was no evidence of hydrogen evolution. Subsequent photolysis experiments were carried out with all the catalysts prepared to establish a comparison among them.

The experimental results obtained are presented in Figs. 4, 5, and 6, where R (extensive hydrogen production rate) is depicted versus t (irradiation time). In all the

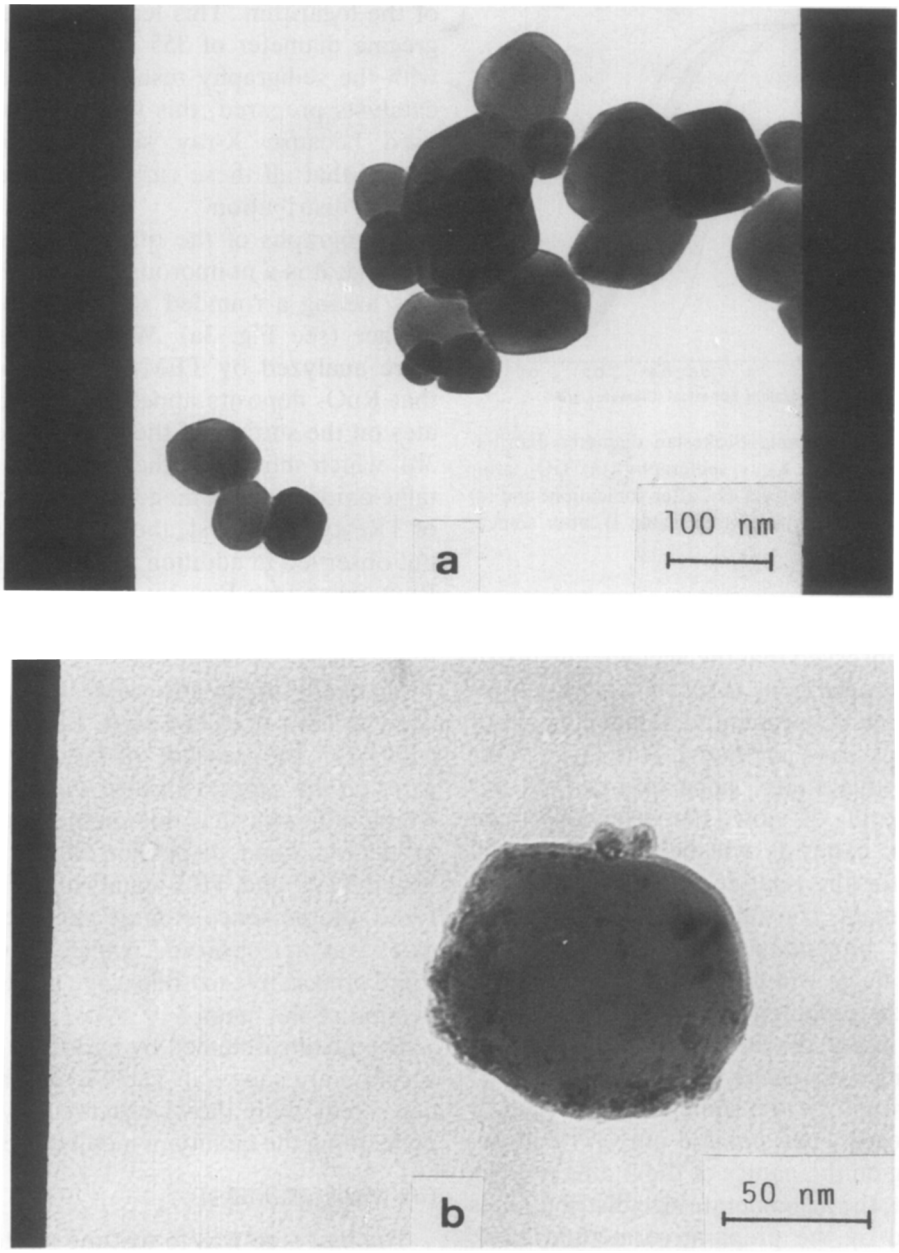

FIG. 3. Transmission electron micrographs: (a) TiO_2; (b) TR catalyst; (c) TRP-type catalysts; (d) TP.C catalyst; (e) TP.H catalyst; (f) TP.F catalyst (see Table 1).

cases studied, it can be seen that the R–t curves show two characteristic zones, a transient period and a pseudo-steady-state period. In the transient period, usually the first 2 or 3 h of irradiation, the hydrogen production rate increases quickly, reaches a maximum and decreases quickly too. After that, the R value decreases very slowly during hundreds of hours and it can be said that a pseudo-steady behavior was observed (this second period will be referred to as the steady zone).

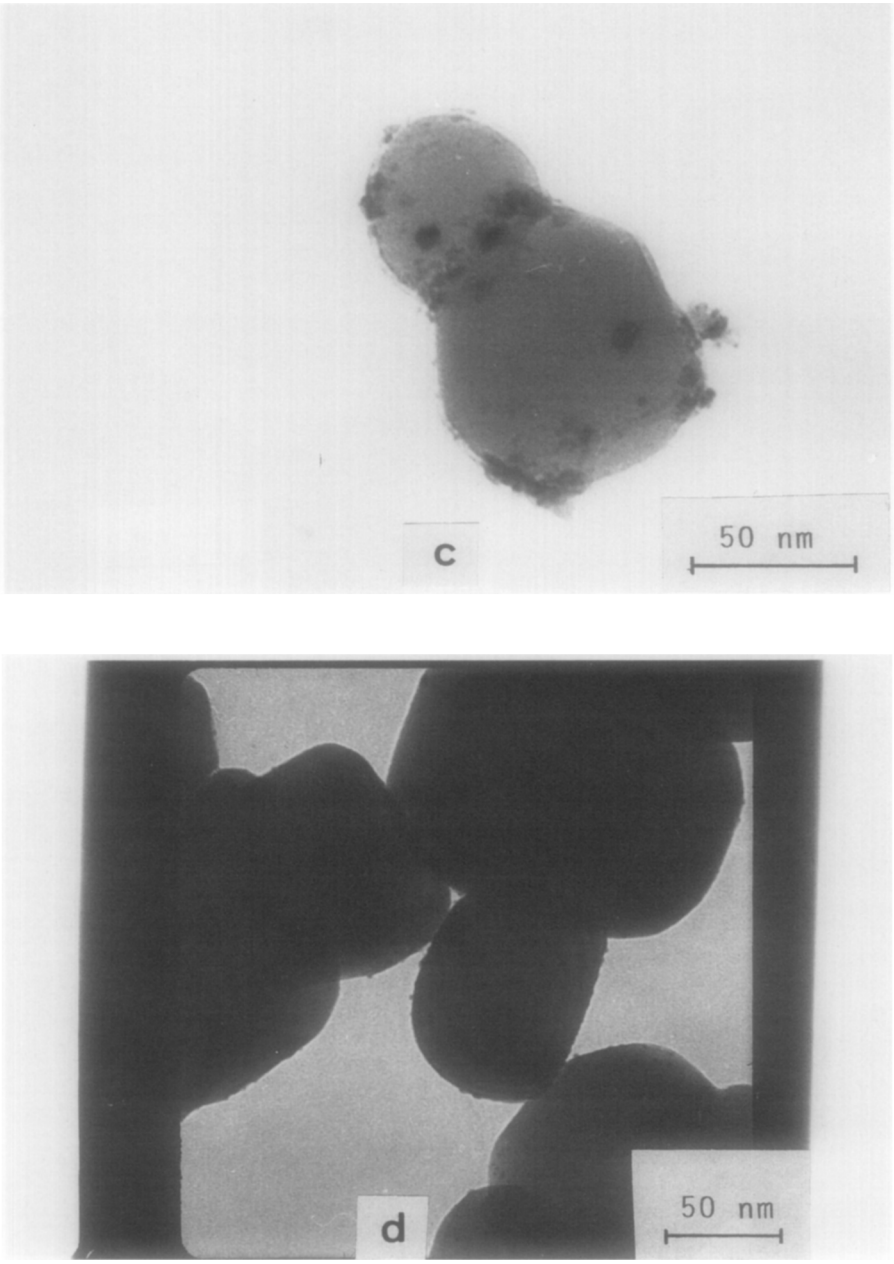

FIG. 3—*Continued*

The experimental results presented in Figs. 4, 5, and 6 are summarized in Table 3. The maximum transient R values as well as the rate values after 17 h of irradiation are presented. After that time the steady zone had been reached in all cases. The cumulative hydrogen production (G) is also given for the same irradiation time.

The behavior of type TP catalysts (Fig. 4, right) is compared to those of type TRP (Fig. 4, left). In addition, the three platinum deposition methods, viz., citrate (C), hy-

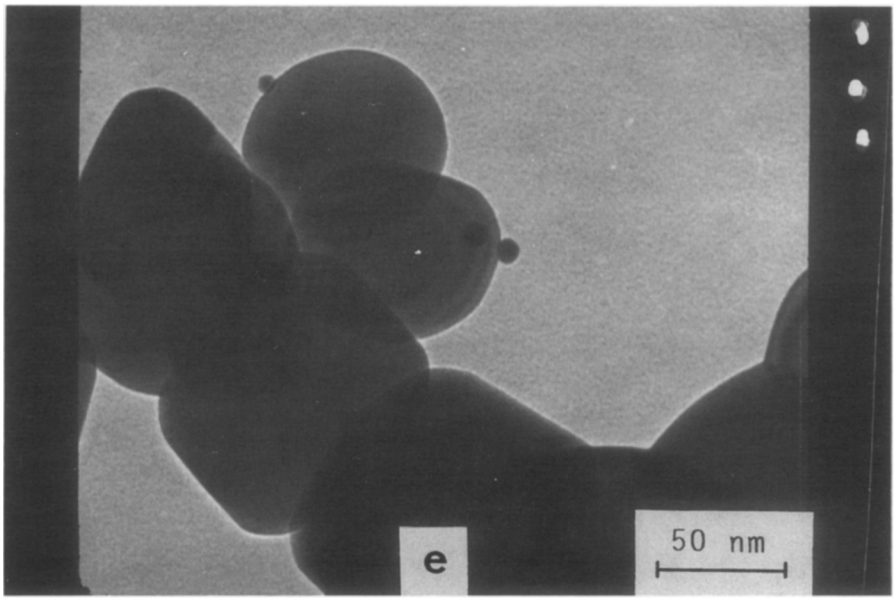

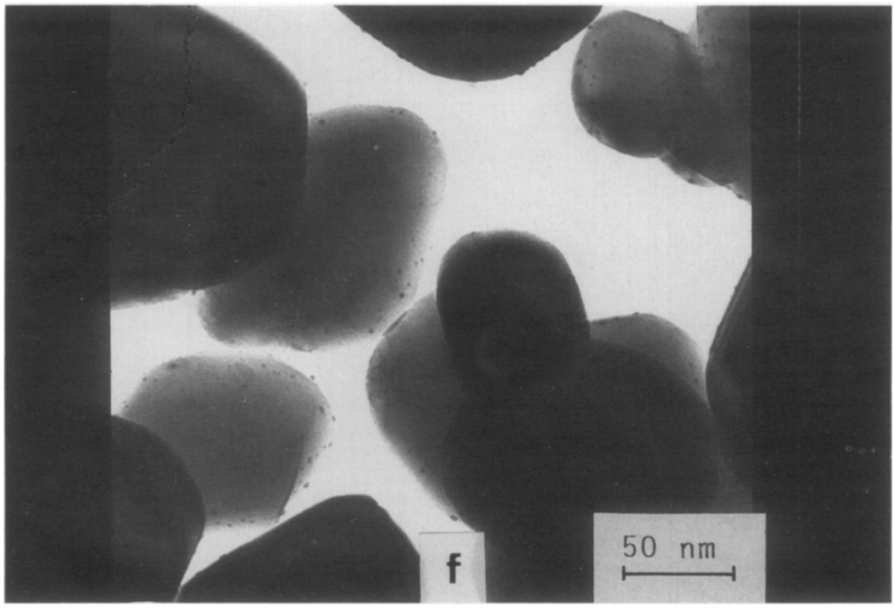

FIG. 3—*Continued*

drogenation (H), and photoplantinization (F), can also be compared for each catalyst type. The citrate-treated catalysts exhibit a greater activity decrease along the steady period. The best results concerning production and stability are given by TRP.H, TRP.F, and TP.F catalysts, where the first of them presents the highest maximum rate. The steady rate is similar for these three catalysts. Ruthenium does not improve the activity of TRP.C and TRP.F compared to TP.C and TP.F. Differences are only ob-

TABLE 2

Metal Dispersion Determined by Hydrogen Chemisorption

Catalysts	Pt dispersion (H/Pt)	Ru dispersion (H/Ru)
TRP.C	0.55	0.04
TRP.H	0.11	0.10
TP.H	0.07	—
TP.F	0.70	—
TR	—	0.04
TR.H	—	0.10

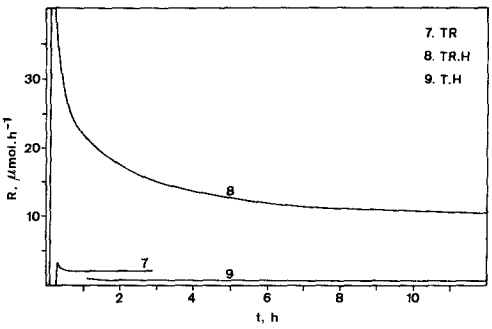

FIG. 5. Hydrogen generation rates (R) vs irradiation time (t) obtained with the catalysts indicated (see Table 1): Influence of the RuO_x deposits.

served in those catalysts which have been hydrogenated.

To analyze the latter observation some experiments were done (Fig. 5) where catalysts without Pt were tested. It can be seen that the hydrogenation at 400°C greatly improves the activity of the TR catalyst. Additionally, pure TiO_2 subjected to hydrogenation shows a constant, although very small, activity with the irradiation time (17 h) in contrast with the nontreated titania.

The most active catalysts (TRP.H, TRP.F, and TP.F) were tested again to study their stabilities. Figure 6 shows the behavior of these catalysts. A first irradiation (left part of Fig. 6) was followed by an Ar flush in the dark (2 ml/s for 3 h) and a second irradiation (right part of Fig. 6). It can be seen that the values of R in the steady period remain constant for the whole testing, and that transients are reproduced after the flush. All three catalysts present steady rates very close to each other, as shown previously in comparative experiments (Fig. 4 and Table 3).

Further experiments carried out with TRP.H and TP.F catalysts made clear that the activity of these catalysts remains constant for at least 1 week of continuous irradiation. However, the activity of the catalysts prepared by the citrate method shown in a first irradiation is not recovered in a second irradiation after the Ar flush; the catalysts lose more than two-thirds of their activity for an irradiation period of 40 h.

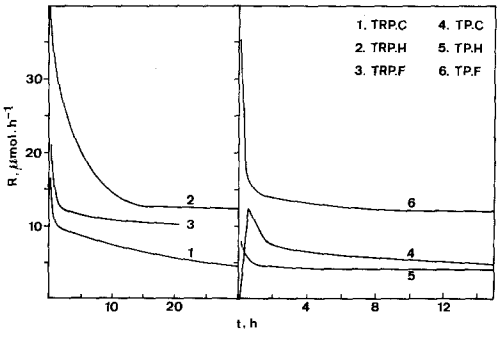

FIG. 4. Hydrogen generation rates (R) vs irradiation time (t) obtained with the catalysts indicated (see Table 1): Effect of the Pt reduction method.

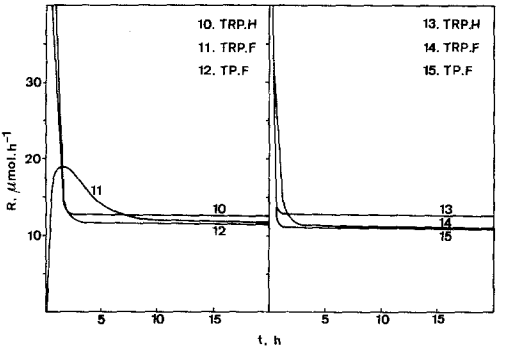

FIG. 6. Hydrogen generation rates (R) vs irradiation time (t) obtained with the catalysts indicated (see Table 1): Stability test. (Left) First irradiation; (right) second irradiation after turning off and flushing Ar.

TABLE 3

Hydrogen Production Rates Obtained in Testing the Different Catalysts in Water Photolysis Experiments

Expt.	Catalyst	R_{max} (μmol/h)	R_{17}[a] (μmol/h)	G_{17}[b] (μmol)
1	TRP.C	16.3	6.0	140
2	TRP.H	63	12.2	332
3	TRP.F	21	10.8	197
4	TP.C	12.2	4.6	100
5	TP.H	7.8	4.1	71
6	TP.F	35	11.5	229
7	TR	3.2	2.0[c]	—
8	TR.H	56	10.4	225
9	T.H	0.8	0.6	10
10	TRP.H	85	12.5	252
11	TRP.F	19.0	11.7	225
12	TP.F	41	11.6	224
13	TRP.H	110	12.6	244
14	TRP.F	36	11.2	217
15	TP.F	77	10.8	193

[a] R_{17}: Hydrogen production rate after 17 h of irradiation.

[b] G_{17}: Cumulative production after 17 h of irradiation.

[c] Rate after 2.4 h of irradiation.

DISCUSSION

The type of test and representation used here enables the evolution of hydrogen with time to be described more accurately than by the cumulative hydrogen production (G) curves. The latter has been applied by most authors using data obtained in batch reactors. Certainly, the hydrogen rate for each t-value can be obtained from the corresponding slope of the G–t curve, but with a significant inaccuracy. Here, it is calculated directly from flow rate and concentration measurements of the continuous gas phase. On the other hand, the gathering of photoproducts in batch reactors increases largely the back-reaction rate (*32*), depriving the results of meaning. In addition, R–t plots enable us to compare the activity of different catalysts in the transient period and in the steady period separately. This is an important feature, because the reproducibility of the steady period is much better than that of the transient period, as shown in Table 3 when R_{max} and R_{17} values of equivalent experiments are compared, respectively. Further, for the catalysts prepared "*in situ*" by photoplatinization, the first transient period takes longer (see Fig. 6, left) and the corresponding R_{max} value is lower than that obtained after an Ar flush once the photoplatinization process was accomplished (see Fig. 6, right).

Complex phenomena, not yet well established, take place in the transient period (*21, 28, 38–42*). The catalyst surface is initially free of photoproducts and shows great activity after a short induction period. The hydrogen generated by the photolytic process diffuses into the catalyst bulk (*43*): on the one hand, an increase in the donor density is produced and, on the other hand, the Pt/TiO_2 barrier becomes ohmic (*44*). Thus, the photolytic activity reaches a maximum quite suddenly at the end of this inductive period and decreases probably due to the covering of titania surface by peroxides.

A tentative mechanism (Fig. 7) can be worked out based on the findings of other authors and our experimental evidence about what could be called an "oxygen trap" where hydrogen peroxide is involved. Given that at the very beginning of the process our suspensions were oxygen free, the initial reactants are H^+ and OH^-. Once the reactants have been adsorbed, protons undergo e_{CB} reduction and eventually produce hydrogen (reactions 1 to 4, Fig. 7). Hydroxyl ions, on the other hand, are oxidized by h_{VB}, yielding adsorbed hydrogen peroxide (reactions 5 to 7, Fig. 7). This species can be either reduced by e_{CB} to yield OH^- to the solution (reaction 8, Fig. 7) or oxidized to oxygen, which will be subsequently photoadsorbed to O_2^- and to O_2^{2-} and eventually converted to adsorbed hydrogen peroxide under the effect of protons (reactions 9 to 12, Fig. 7). An alternate path to the elimination of adsorbed H_2O_2 is its desorption to the liquid phase (reaction 13,

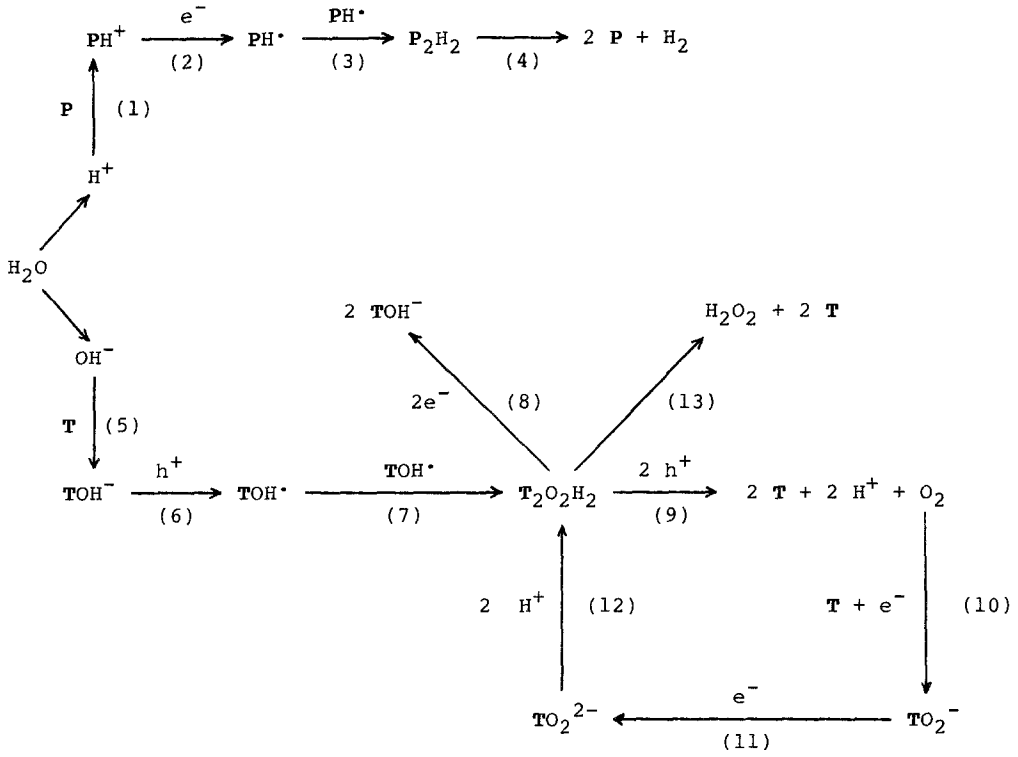

FIG. 7. Reaction network. P represents platinum sites and T denotes titanium surface sites, where different species can be adsorbed or react (see text for further explanation).

Fig. 7). Once dissolved, the simultaneous presence of UV light and Pt would lead to this hydrogen peroxide decomposition, where the oxygen evolved could leave the liquid phase either via the gas phase or by photoadsorbtion. This scheme could explain why it is so difficult to detect oxygen in the gas phase; there is an oxygen trap in the form of hydrogen peroxide attached to the solid surface. The amount of hydrogen peroxide that can be held by the solid on its surface has been assessed by Harbour *et al.* (*41*) to be of the order of some 20 monolayers. These peroxides did not migrate to the interior of the semiconductor in our experiments, for XRD of long-irradiated catalysts did not show any crystallinity loss that could be originated by the conversion of the TiO_2 lattice into amorphous hydroperoxy species. On the other hand, irradiated powders slowly evolved hydrogen peroxide from the surface in the dark, this H_2O_2 being detected by the horseradish peroxidase method, which is a specific test for hydrogen peroxide.

The steady state eventually reached depends on the radiation flux field, the catalyst type and the mass transfer through the liquid–gas interface (*34*). In this study, the radiation flux and the mass transfer parameters were kept constant, so that the catalyst performances could be checked by the steady-state hydrogen production rate.

When TP type catalysts were tested (Fig. 4, right), the differences observed in their behavior can be attributed to the preparative method used, because the support characteristics and the catalyst concentration are the same in all cases. It can be seen that hydrogen production is greater when the dispersion of Pt loaded on the support is better (Table 2 and Figs. 3d, 3e, and 3f)

(*22*). In this case, the highest production was shown by the catalysts prepared by the photoplatinization method. However, the performance of the TP.H catalyst was better than expected, considering that the Pt dispersion was so poor, according to its H/Pt ratio.

The situation seems to be different when catalysts were loaded with RuO_2. These surface deposits do not improve the activity of the catalysts prepared by the citrate method or by photoplatinization, as stated before, but they do improve it when catalysts are prepared by hydrogenation. Certainly, the pure RuO_2 is catalytically active. In fact, Fig. 5 shows that when titania is loaded with RuO_2 (catalyst TR, see Table 1), hydrogen production is observed. This proves that RuO_2 can be thought of as an active catalyst in the water photolysis process, but its catalytic efficiency is much lower than that of the TP catalysts tested (Fig. 4, right) (*7*, *45*).

A sound explanation of this apparent contradiction would be that when Pt (on RuO_2/TiO_2) is reduced also by the hydrogenation method, part of the RuO_2 present would be reduced and this reduced ruthenium would perform as a better catalyst than RuO_2 in the photoreduction of H^+ to H_2 in the water photolysis process. This is in agreement with the fact that when a TR catalyst is subjected to the same hydrogenation process, the resulting TR.H catalyst is much more active than the preceding form (see Fig. 5). Ruthenium originating from RuO_2 reduction with hydrogen is an active catalyst in reducing protons, and that is why the steady hydrogen production of the TR.H catalyst is comparable to that of other catalysts containing platinum. On the other hand, RuO_2 is not a good reduction catalyst if used as it is loaded on the support (see Fig. 5, expt. 7).

Another factor to take into account would be the change that the titania support undergoes in the hydrogenation treatment. As shown in Fig. 5, titania hydrogenated at 400°C becomes photolytically active, in contrast with the untreated form. This treatment is like a doping, increasing its donor density and promoting significant changes in the spectral response, understood in terms of process quantum yield enhancement (*47*). Titania hydrogenated at high temperature contains OH^- anions close to Ti^{3+} cations in the crystal network, without creating structural disorder (*46*). On the contrary, the conductivity produced by diffusion of hydrogen atoms (generated, for example, photocatalytically on the catalyst surface) into the TiO_2 bulk at room temperature is ascribed to the electron transfer from interstitial hydrogen atoms to the conduction band and the consequent production of interstitial H^+ (*43*). Lattice site donors migrate much more slowly than interstitial ones, and so the resultant material from the high-temperature treatment should be more stable. The hole mean life is longer and the electron–hole recombination is diminished.

The hydrogenated catalysts present a support-tied characteristic, namely, their greater stability. The actual *R*-values can depend on factors such as the dispersion degree of the metal on the surface of the support. This could explain why TP.F and TP.C catalysts present *R*-values higher than TP.H, although the stability of the latter is greater.

It can be concluded that RuO_2 itself, while remaining as an oxide, has no significant influence on the hydrogen production rate, and the differences observed between TP.H and TRP.H catalysts can be attributed to the reduction of RuO_2 and the doping of TiO_2, both phenomena being promoted by the thermal treatment in hydrogen. The increase in the lattice site donors originated by this treatment would also explain the relatively good performance of TP.H catalyst despite its worse Pt dispersion.

Finally, the worse stability of the catalysts prepared by the citrate method could be caused by the different contacts existing between Pt and TiO_2 when Pt either comes

from a colloid or is reduced *in situ* at the support surface (*48*). The adherence of the Pt deposits obtained by the citrate method could decrease with the irradiation time, mainly due to mechanical factors acting at the catalyst surface.

ACKNOWLEDGMENTS

The authors are grateful to CAICYT (657/81 and 705/84), to "Caixa de Barcelona," and to the University of Barcelona for funds received to carry out this work. The authors are also grateful to the Electron Microscopy Service of the University of Barcelona, to the "Jaume Almera" Institute of CSIC, and to Mrs. E. Bastús of the Chemical Technology Department of the Catalonia Politechnique University for valuable collaboration in the characterization of the catalysts.

REFERENCES

1. Grätzel, M., "Energy Resources through Photochemistry and Catalysis." Academic Press, New York, 1983.
2. Schiavello, M., "Photoelectrochemistry, Photocatalysis and Photoreactors: Fundamentals and Developments." Reidel, Dordrecht, 1985.
3. Cervera-March, S., and Esplugas, S., *Energía* **9,** 103 (1983).
4. Cervera-March, S., Esplugas, S., and Simarro, R., *Afinidad* **41,** 283 (1984).
5. Foger, K., "Catalysis: Science and Technology" (M. Boudart and J. R. Anderson, Eds.), Springer-Verlag, Berlin, 1984.
6. Moss, R. L., "Experimental Methods in Catalytic Research," Vol. III. Academic Press, New York, 1976.
7. Serpone, N., Borgarello, E. and Grätzel, M., *J. Chem. Soc. Chem. Commun.* **6,** 342 (1984).
8. Ulman, M., Tinnemans, A. H. A., Mackor, A., Aurian-Blajeni, B., and Halmann, M., *Int. J. Sol. Energy* **7,** 213 (1982).
9. Schumacher, E., *Chimia* **32,** 193 (1978).
10. Erbs, W., Desilvestro, J., Borgarello, E., and Graetzel, M., *J. Phys. Chem.* **88,** 4001 (1984).
11. Borgarello, E., and Pelizzetti, E., *Inorg. Chim. Act.* **91,** 300 (1984).
12. Duonghong, D., Borgarello, E., and Grätzel, M., *J. Amer. Chem. Soc.* **103,** 4685 (1981).
13. Kalyanasundaram, K., Borgarello, E., and Grätzel, M., *Helv. Chim. Act.* **64,** 362 (1981).
14. Blondeel, G., Harriman, A., Porter, G., Urwin, D., and Kiwi, J., *J. Phys. Chem.* **87,** 2629 (1983).
15. Borgarello, E., Kiwi, J., Pelizzetti, E., Visca, M., and Graetzel, M., *J. Amer. Chem. Soc.* **103,** 6324 (1981).
16. Borgarello, E., Kalyanasundaram, K., and Grätzel, M., *Helv. Chim. Act.* **65,** 243 (1982).
17. St. John, M. R., Furgala, A. J., and Sammells, A. F., "World Hydrogen Energy Conference, IV, California, June, 1982."
18. Mills, A., and Porter, G., *J. Chem. Soc. Faraday Trans. 1* **78,** 3659 (1982).
19. Mills, A., *J. Chem. Soc. Chem. Commun.*, 367 (1982).
20. Tauster, S. J., Fung, S. C., and Garten, R. L., *J. Amer. Chem. Soc.* **100,** 170 (1978).
21. Kiwi, J., and Grätzel, M., *J. Phys. Chem.* **88,** 1302 (1984).
22. Sato, S., *J. Catal.* **92,** 11 (1985).
23. Duonghong, D., and Grätzel, M., *J. Chem. Soc. Chem. Commun.* **23,** 1597 (1984).
24. Curran, J. S., Domenech, J., Jaffrezic-Renault, N., and Philippe, R., *J. Phys. Chem.* **89,** 957 (1985).
25. Nakahira, T., and Grätzel, M., *J. Phys. Chem.* **88,** 4006 (1984).
26. Allen, T., "Particle Size Measurement," 3rd ed. Chapman and Hall, London, 1981.
27. Gregg, S. J., and Sing, K. S. W., "Adsorption, Surface Area and Porosity," 2nd ed. Academic Press, New York, 1982.
28. Irani, R. R., and Callis, C. F., "Particle Size: Measurement, Interpretation and Application." Wiley, New York, 1963.
29. Gu, B., Kiwi, J., and Grätzel, M., *Nouv. J. Chim.* **9,** 539 (1985).
30. Escudero, J. C., doctoral thesis, University of Barcelona, Barcelona, 1987.
31. Simarro, R., Cervera-March, S., Giménez, J., and Escudero, J. C., *EPA Newslett.* **29,** 35 (1987).
32. Simarro, R., Cervera-March, S., and Esplugas, S., *Int. J. Hydrogen Energy* **10,** 221 (1985).
33. Cervera-March, S., Esplugas, S., and Simarro, R., *Anal. Fis.* **81,** 29 (1985).
34. Escudero, J. C., Giménez, J., Cervera-March, S., and Simarro, R., *Chem. Eng. Sci.* **44,** 583 (1989).
35. Esplugas, S., Cervera-March, S., and Simarro, R., *Chem. Eng. Commun.* **51,** 221 (1987).
36. Chung, F. H., *J. Appl. Crystallogr.* **7,** 519 (1974).
37. Escudero, J. C., Giménez, J., Simarro, R., and Cervera-March, S., *Sol. Energy Mater.* **17,** 151 (1988).
38. Munuera, G., Soria, J., Conesa, J. C., Sanz, J., González-Elipe, A. R., Navio, A., López-Molina, E. J., Muñoz, A., Fernández, A., and Espinós, J. P., *Stud. Surf. Sci. Catal.* **19,** 335 (1984).
39. Muraki, H., Saji, T., Fujihira, M., and Aoyagui, Sh., *J. Electroanal. Chem. Interfacial Electrochem.* **169,** 319 (1984).
40. Yesodharan, E., Yesodharan, S., and Graetzel, M., *Sol. Energy Mater.* **10,** 287 (1984).
41. Harbour, J. R., Tromp, J., and Hair, M. L., *Canad. J. Chem.* **63,** 204 (1985).

42. Salvador, P., *J. Phys. Chem.* **89,** 3863 (1985).
43. Harris, L. A., Gerstner, M. E., and Wilson, R. H., *J. Electrochem. Soc.* **126,** 850 (1979).
44. Hodes, G., and Graetzel, M., *Nouv. J. Chim.* **8,** 509 (1984).
45. Sakata, T., Hashimoto, K., and Kawai, T., *J. Phys. Chem.* **88,** 5214 (1984).
46. Harris, L. A., and Schumacher, R., *J. Electrochem. Soc.* **127,** 1186 (1980).
47. Pleskov, Yu. V., and Gurevich, Yu. Ya., "Semiconductor Photoelectrochemistry." Consultants Bureau, New York, 1986.
48. Nosaka, Y., Ishizuka, Y., and Miyama, M., *Ber. Bunsenges. Phys. Chem.* **90,** 1199 (1986).